MOSBR
Molecular-Scale Biophysics Research Infrastructure

Applications of EPR spectroscopy to the study of metalloproteins

Stéphane GRIMALDI

Laboratory of Bioenergetics and Protein Engineering
CNRS / Aix-Marseille Université
Marseille - France

Aix*Marseille université

Bioénergétique et Ingénierie des Protéines

cnrs advancing the frontiers

This project has received funding from the European Union's Horizon 2020 research and innovation programme under grant agreement No 101004806

Outline

- Magnetic properties of metallic prosthetic groups

  Iron, low spin (S = ½) *vs* high spin (S = 5/2) hemes, polynuclear FeS clusters

- Origin and spectral effect of hyperfine couplings

  Copper, molybdenum

- Analysis of EPR spectral amplitudes/intensities

  Spin quantitation, EPR-monitoring of (i) redox reactions,
  (ii) binding experiments
  (iii) kinetics

- Examples of (advanced) EPR experimental strategies
  Selective detection of metal centres in multicentre metalloproteins
  Multifrequency experiments,
  Complementing cw EPR with hyperfine spectroscopy

This project has received funding from the European Union's Horizon 2020 research and innovation programme under grant agreement No 101004806

Metals in biology

- Metals are essential in biology

Transition metal = partially filled *d* orbitals

Transition metals with biological function

This project has received funding from the European Union's Horizon 2020 research and innovation programme under grant agreement No 101004806

EPR-active oxidation states of transition metals ions

Metal	Main biological functions	EPR-active oxidation states
Iron (Fe)	Oxidase, oxygen transport and storage, electron transfer, nitrogen fixation	Fe(II) Fe(III) Fe(IV)
Copper (Cu)	Oxidase, oxygen transport, electron transfer	Cu(II)
Manganese (Mn)	Photosynthesis, oxidase, structure	Mn(II) Mn(III) Mn(IV)
Nickel (Ni)	Hydrogenase, hydrolase	Ni (I) Ni (II) Ni (III)
Molybdenum (Mo)	Nitrogen fixation, oxidase, oxygen transfer,…	Mo(V)
Cobalt (Co)	Oxidase, transfert of alkyl groups	Co(II)
Tungstene (W)	Dehydrogenase, CO_2 reduction	W(V)
Vanadium (V)	Nitrogen fixation, oxidase	V(III)

Hydrolase: $R\text{-}R' + H_2O = R\text{-}OH + R'H$

Alkyl groups: C_nH_{2n+1}

This project has received funding from the European Union's Horizon 2020 research and innovation programme under grant agreement No 101004806

Magnetic properties of mononuclear metal cofactors

Example: Free Fe, Fe^{2+}, Fe^{3+}

26
Fe
Iron
55.85

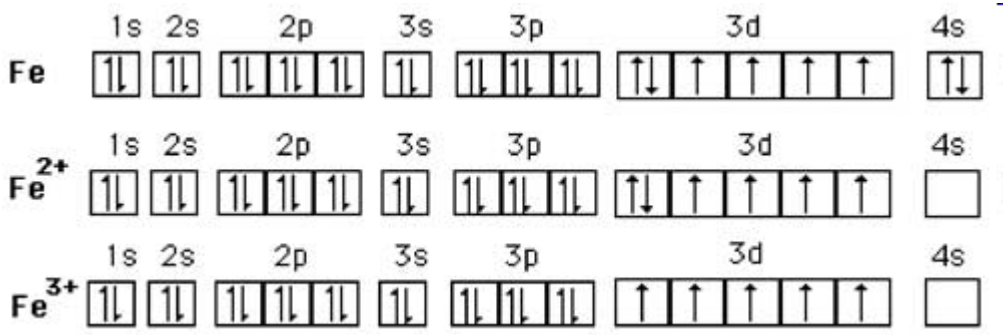

reduction →

$Fe^{3+} + 1e^- = Fe^{2+}$

← oxidation

[Ar] $3d^6\ 4s^2$: S = 4 x ½ = 2

[Ar] $3d^6$: S = 4 x ½ = 2

[Ar] $3d^5$: S = 5 x ½ = 5/2

} EPR-active

Half integer spins: perpendicular mode detection
Integer spins: parallel mode detection

This project has received funding from the European Union's Horizon 2020 research and innovation programme under grant agreement No 101004806

Magnetic properties of mononuclear metal cofactors

- The energy of the d orbitals are modified by the presence of ligands and their nature
- Ligand field approach: Magnetic properties mainly due to *d* electrons

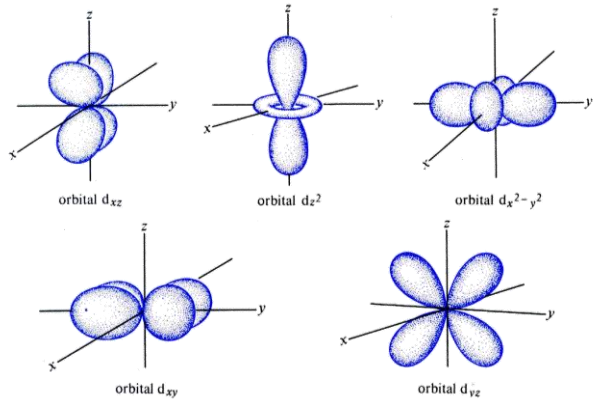

Example: Fe^{3+}

[Ar] $3d^5$

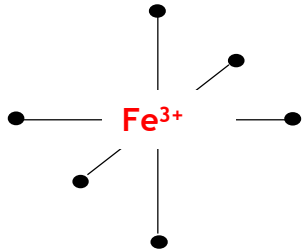

Octahedral geometry

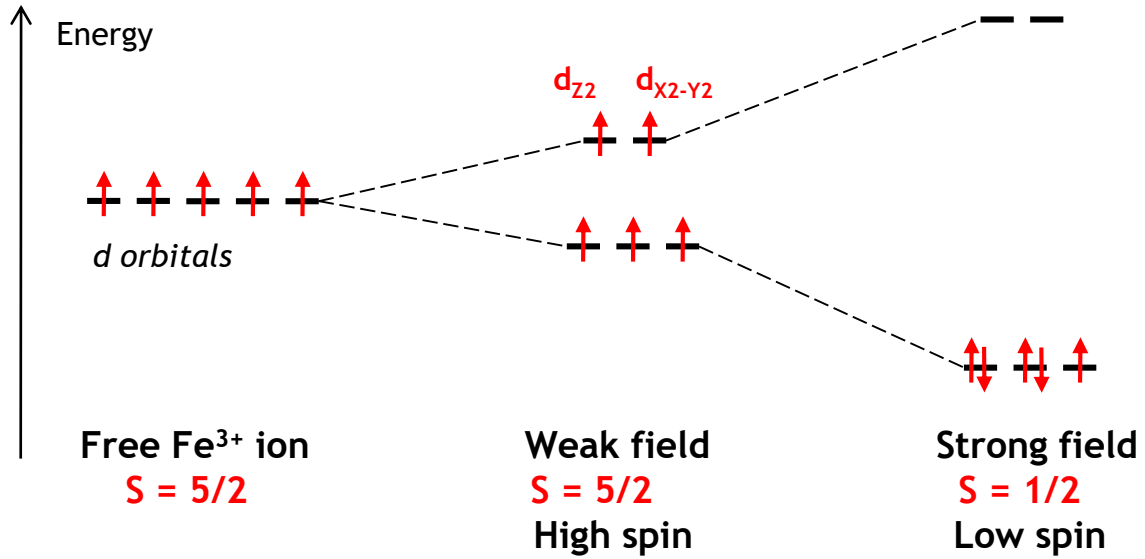

Heme in Myoglobine

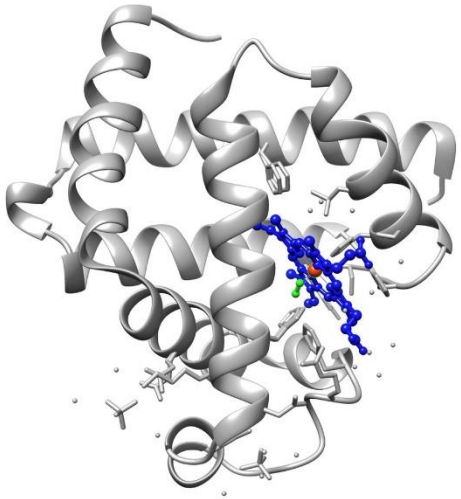

This project has received funding from the European Union's Horizon 2020 research and innovation programme under grant agreement No 101004806

Magnetic properties of mononuclear metal cofactors

- Example: EPR spectra of myoglobin in the presence/absence of azide (N_3^-)

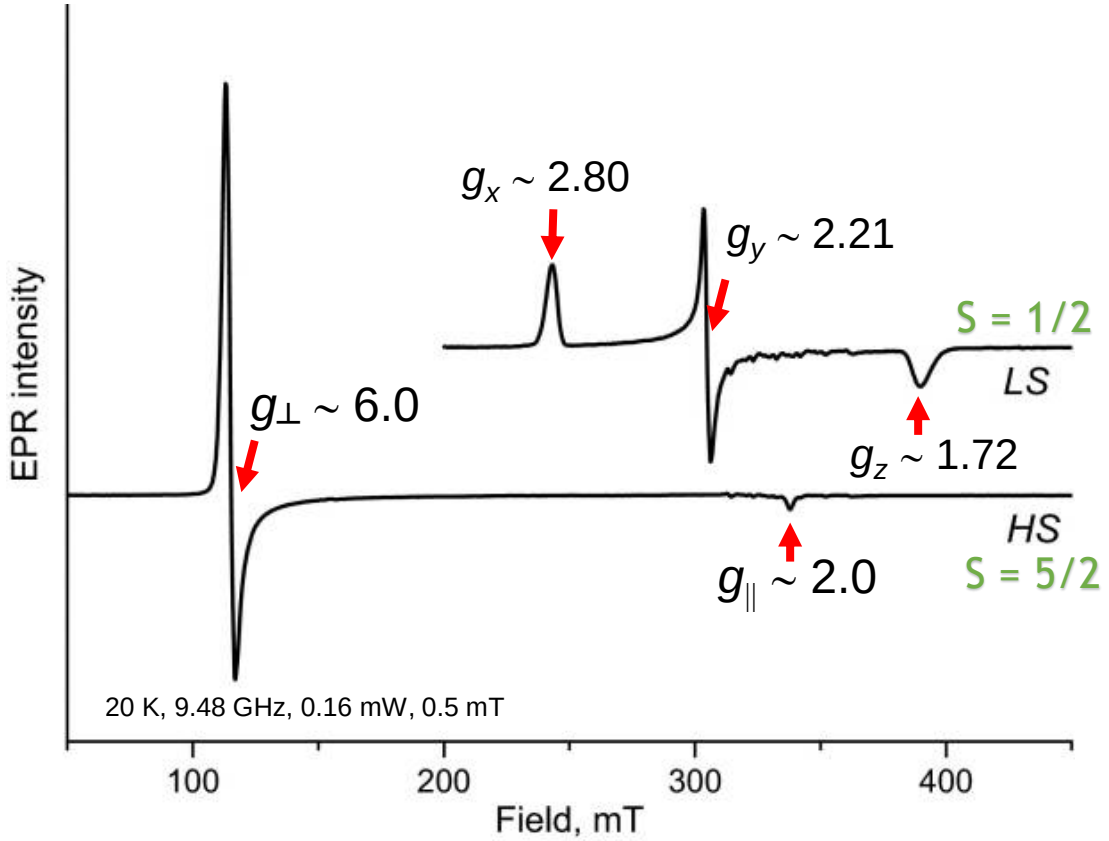

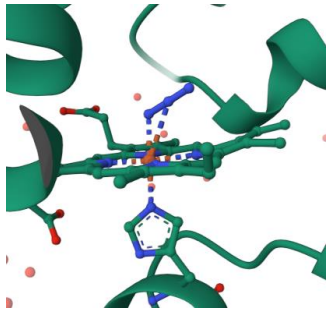

Myoglobin + azide

PdB 1SWM

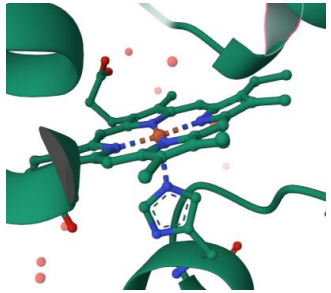

Myoglobin

PdB 1VXA

See practical session P2

Nami et al. (2016) Appl Magn Reson

This project has received funding from the European Union's Horizon 2020 research and innovation programme under grant agreement No 101004806

Magnetic properties of S = ½ metal cofactors

Spin hamiltonian: $H_{spin} = \beta \vec{S} \tilde{g} \vec{B}$

e.g., LS Fe^{3+}

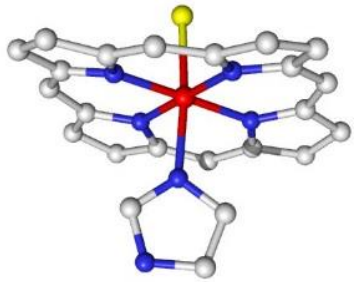

Anisotropic $\tilde{g}$ tensor:

- (*X*, *Y*, *Z*) principal axes of *g*:
- (g_X, g_Y, g_Z) principal g-values

Magnetic axes are related to symmetry axes and atomic positions (= molecular axes)

The line position ***g' depends on the $\vec{B}$ orientation***

$$g'^2 = l_X^2 g_X^2 + l_Y^2 g_Y^2 + l_Z^2 g_Z^2$$

$$g'^2 = \cos^2\varphi \cdot \sin^2\theta \, g_X^2 + \sin^2\varphi \cdot \sin^2\theta \, g_Y^2 + \cos^2\theta \, g_Z^2$$

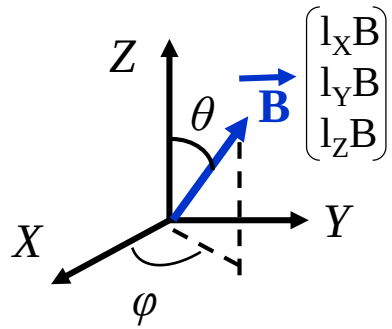

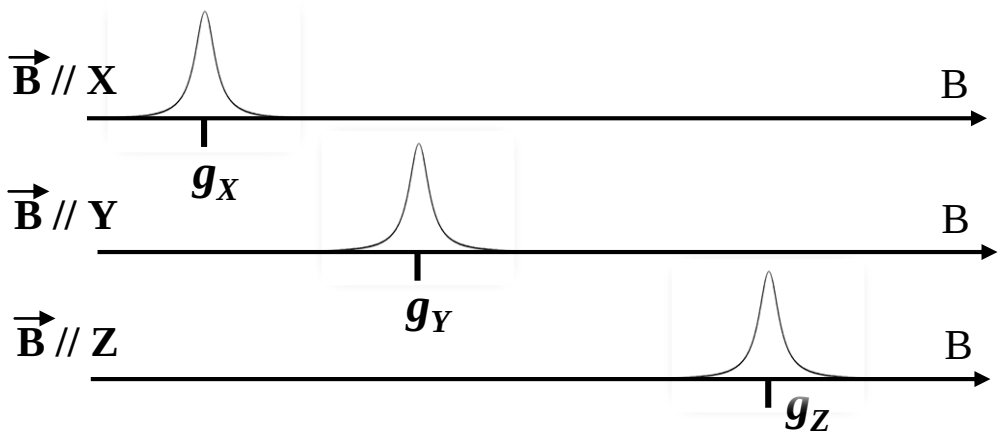

This project has received funding from the European Union's Horizon 2020 research and innovation programme under grant agreement No 101004806

Magnetic properties of S = ½ metal cofactors

Anisotropic *g* tensor- Powder or frozen solution spectrum (metalloproteins at cryogenic temperatures)

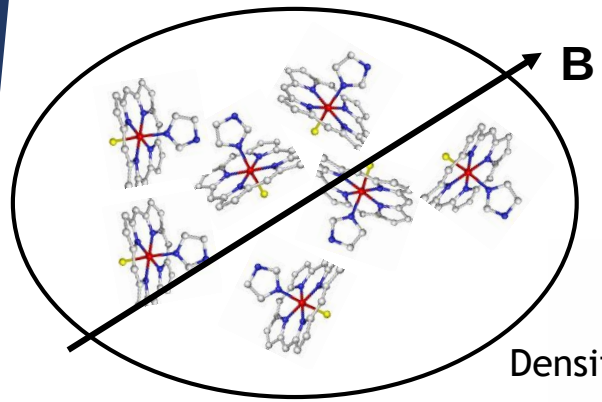

Disordered system: all the B orientations are sampled

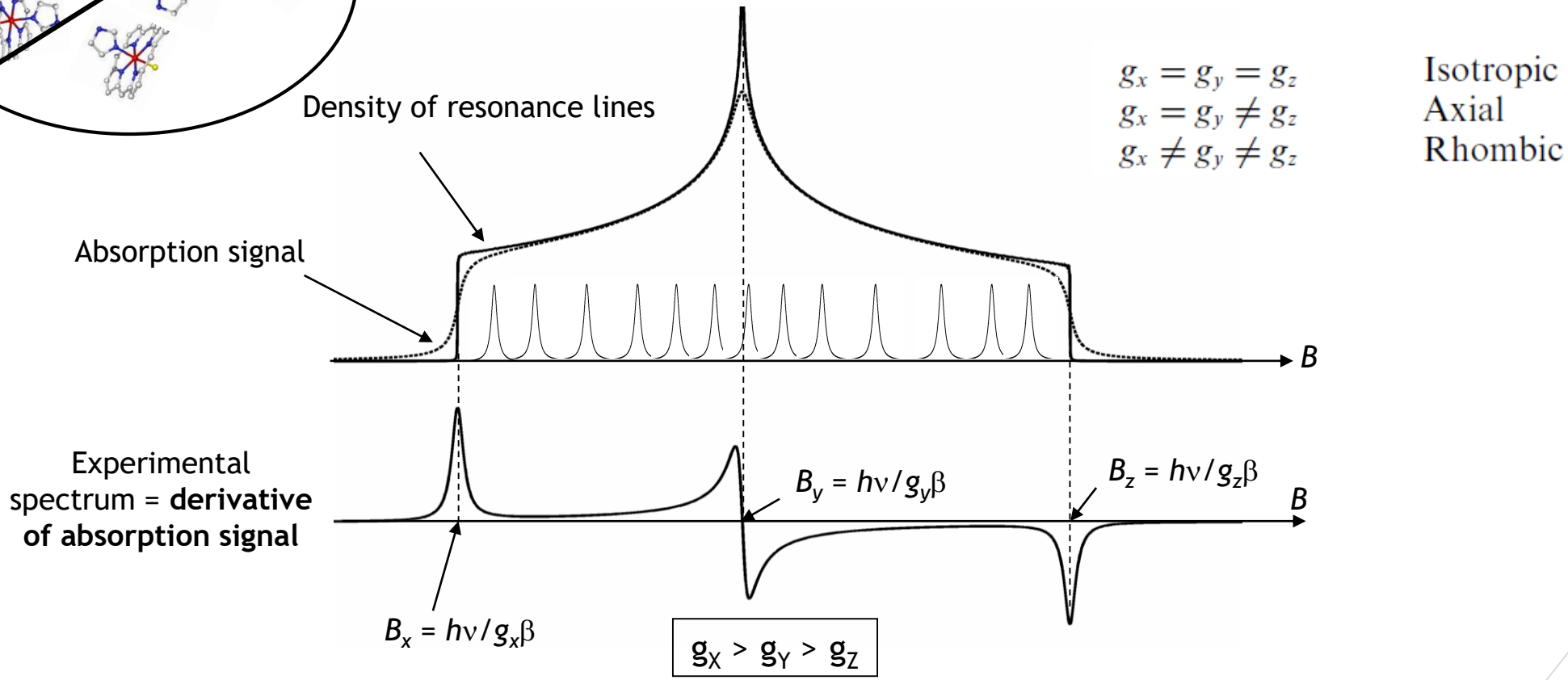

$g_x = g_y = g_z$ Isotropic
$g_x = g_y \neq g_z$ Axial
$g_x \neq g_y \neq g_z$ Rhombic

This project has received funding from the European Union's Horizon 2020 research and innovation programme under grant agreement No 101004806

Magnetic properties of S = 5/2 metal cofactors

S = 5/2 , M_S = -5/2, -3/2, -1/2, +1/2, +3/2, +5/2: 6 states {|**S, M_S**>}

Influence of fine structure (Zero field splitting) due to interactions between unpaired electrons

$$H_{spin} = \vec{S}\tilde{D}\vec{S} + \beta\vec{S}\tilde{g}\vec{B}$$

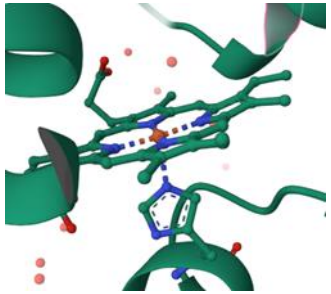

D axial, ***g*** isotropic (= *g*) (e.g. HS Fe^{3+} in myoglobin)

Case **D >> g ß B** **(0.3 cm^{-1} at 0.3 T)**

B = 0 : Zero field splitting

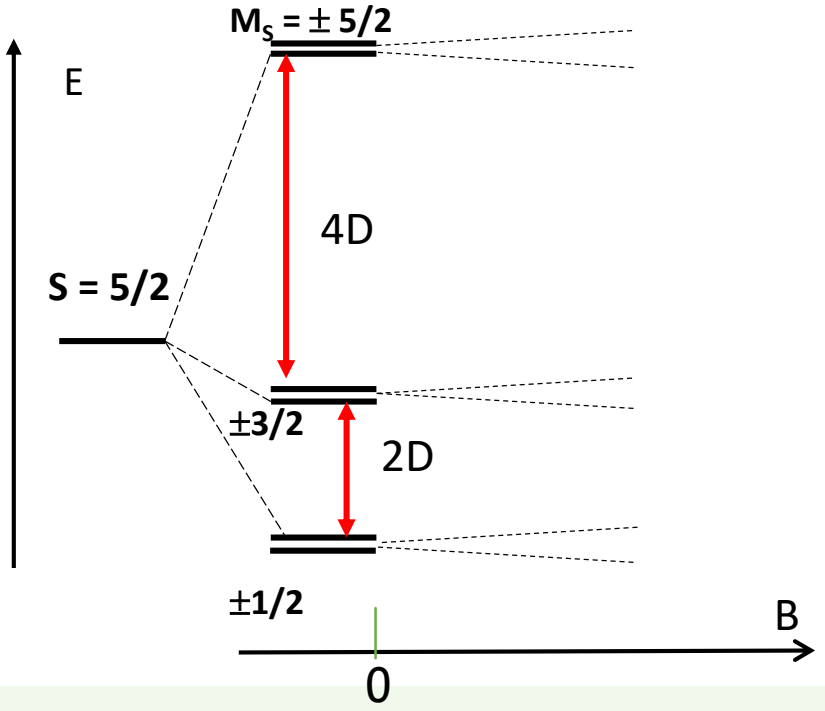

This project has received funding from the European Union's Horizon 2020 research and innovation programme under grant agreement No 101004806

Magnetic properties of S = 5/2 metal cofactors

Axial symmetry- **D >> g ß B**

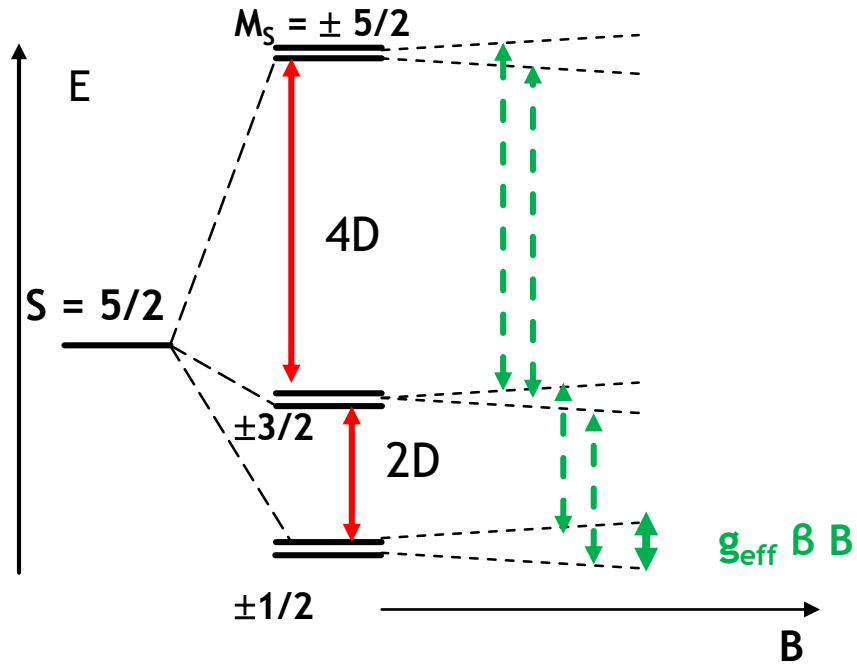

g_{eff} ß B

5 allowed EPR transitions $\Delta M_S = \pm 1$

Only one is energetically accessible :

$h\nu \approx g\beta B << D$

$M_S = \pm 1/2$ g_{eff} **axial :** $g_{eff\,//} = g = 2$, $g_{eff\perp} = 3g = 6$

Axial spectrum

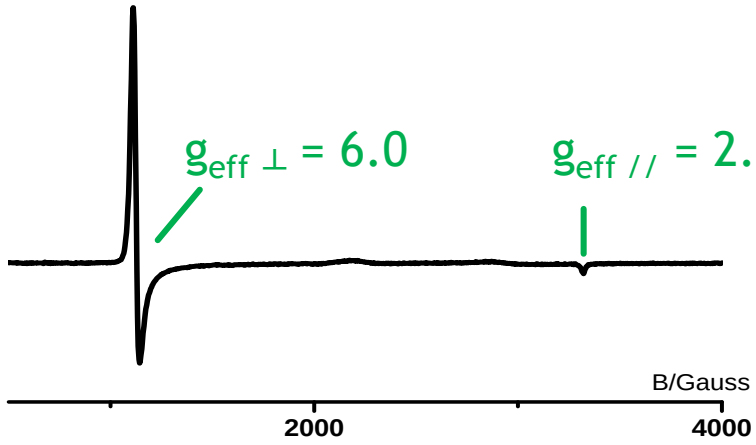

This project has received funding from the European Union's Horizon 2020 research and innovation programme under grant agreement No 101004806

Magnetic properties of polynuclear metal clusters

- Example: « conventional » FeS clusters

➡ Magnetic properties arise from (exchange) coupling between Fe^{3+} (S = 5/2) and Fe^{2+} (S = 2) ions

Structure	Main oxidation states [a,b]	Spin state (ground state)	Redox state of individual Fe atoms
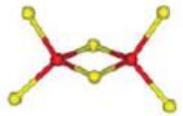	$[2Fe\text{-}2S]^{2+}$ $[2Fe\text{-}2S]^{+}$	S = 0 S = 1/2	2 x Fe^{3+} Fe^{3+}, Fe^{2+}
	$[3Fe\text{-}4S]^{+}$ $[3Fe\text{-}4S]^{0}$	S = 1/2 S = 2	3 x Fe^{3+} 2 x Fe^{3+}, Fe^{2+}
	$[4Fe\text{-}4S]^{3+}$ $[4Fe\text{-}4S]^{2+}$ $[4Fe\text{-}4S]^{+}$	S = 1/2 S = 0 S = 1/2 or 3/2	3 x Fe^{3+}, 1 x Fe^{2+} 2 x Fe^{3+}, 2 x Fe^{2+} 1 x Fe^{3+}, 3 x Fe^{2+}

[a] Overall charge of the cluster (each sulfide contributes two negative charges), [b] other oxidation states are possible in specific systems

Typical Fe-S EPR signals

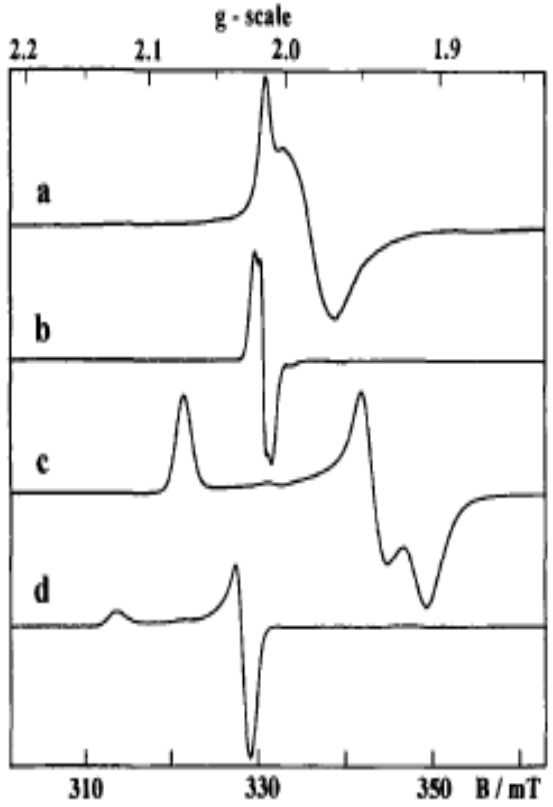

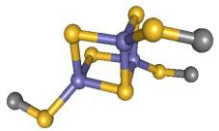

$[3Fe\text{-}4S]^{1+}$
S = 1/2

Fdx $[4Fe\text{-}4S]^{1+}$
S = 1/2

HiPIP $[4Fe\text{-}4S]^{3+}$
S = 1/2

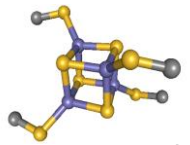

This project has received funding from the European Union's Horizon 2020 research and innovation programme under grant agreement No 101004806

Origin and spectral effect of hyperfine couplings

- Bio transition metal nuclear spins and EPR hyperfine patterns

Metal	Valency	Isotope	Spin (abundance)	EPR lines
V	IV	51	7/2	8
Mn	II	55	5/2	6
Fe	III	54, 56, *57*, 58	0 + *1/2* (2%)	1 + 2 (1%)
Co	II	59	7/2	8
Ni	III,I	58, 60, *61*, 62, 64	0 + *3/2* (1%)	1 + 4 (0.25%)
Cu	II	63, 65	3/2	4
Mo	V	92, 94, *95*, 96, *97*, 98, 100	0 + *5/2* (25%)	1 + 6 (4%)
W	V	180, 182, *183*, 184, 186	0 + *1/2* (14%)	1 + 2 (7%)

Nuclear spin I

(2I+1) EPR lines

→ Large » Hyperfine splitting

- Bio ligand atom nuclear spins and EPR superhyperfine patterns

Ligand	Isotope	Spin (abundance)	EPR lines
H	1, 2	1/2 + 1 (0.015%)	2 + 3
C	12, *13*	0 + *1/2* (1.1%)	1 + 2
N	14, *15*	1 + *1/2* (0.4%)	3 + 2
O	16, *17*, 18	0 + *5/2* (0.04%)	1 + 6
F	19	1/2	2
P	31	1/2	2
S	32, *33*, 34	0 + *3/2* (0.8%)	1 + 4
Cl	35, 37	3/2	4
As	75	3/2	4
Se	76, *77*, 78, 80, 82	0 + *1/2* (7.6%)	1 + 4
Br	79, 81	3/2	4
I	127	5/2	6

First coordination sphere

vs.

Higher sphere

(generally unresolved, contribute to the inhomogeneous line width)

Hagen (2006) Dalton Trans.

This project has received funding from the European Union's Horizon 2020 research and innovation programme under grant agreement No 101004806

Anisotropic hyperfine couplings: spectral effects

$$H_S = \vec{S}\,\tilde{D}\,\vec{S} + \beta\,\vec{S}\,\tilde{g}\,\vec{B} + \vec{S}\,\tilde{A}\,\vec{I}$$

- General case: anisotropic ***g*** and ***A*** tensors
  => (2I+1) hyperfine components for each principal direction of ***g***

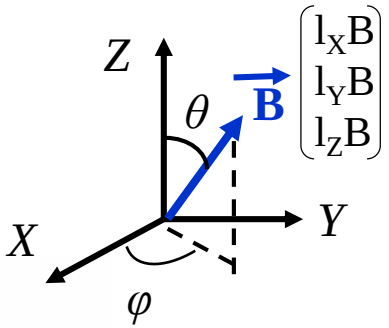

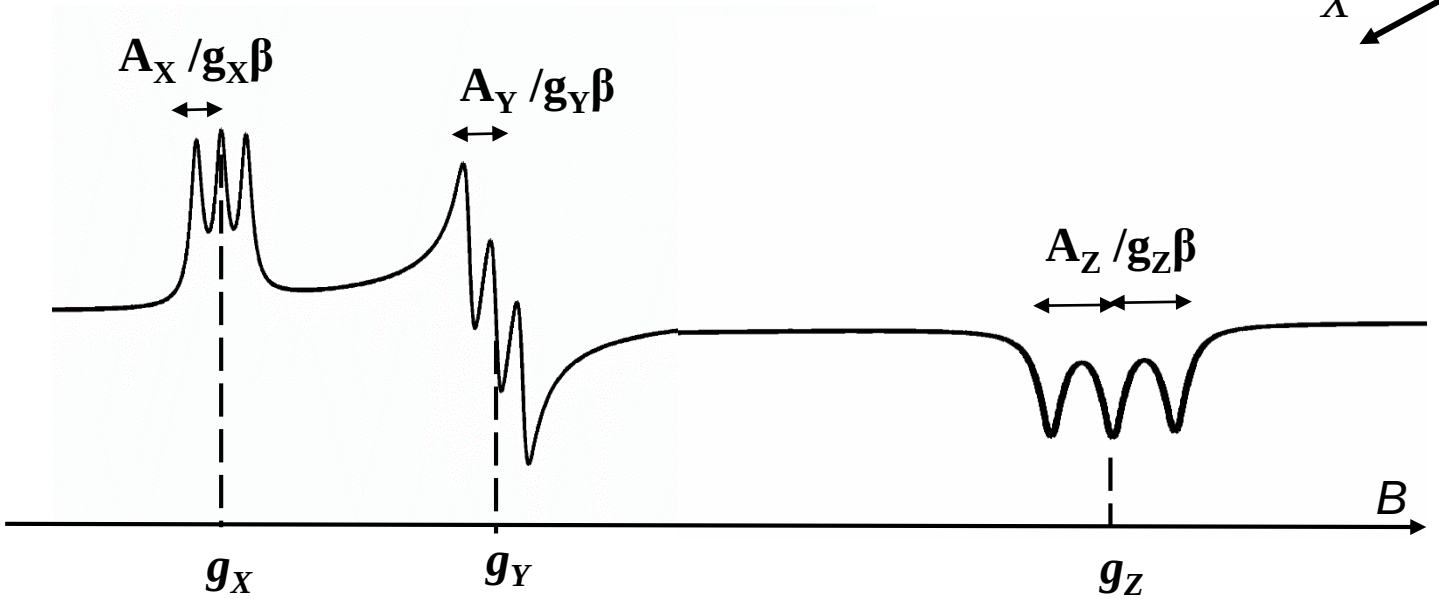

Hyp: ***A*** - and ***g***- tensors with parallel axes

$$g^2 = l_X^2\, g_X^2 + l_Y^2\, g_Y^2 + l_Z^2\, g_Z^2$$

$$A^2 g^2 = l_X^2\, A_X^2 g_X^2 + l_Y^2\, A_Y^2 g_Y^2 + l_Z^2\, A_Z^2 g_Z^2$$

This project has received funding from the European Union's Horizon 2020 research and innovation programme under grant agreement No 101004806

Anisotropic hyperfine couplings: spectral effects

- General case: anisotropic ***g*** and ***A*** tensors

Example of copper enzymes
Cu (Z = 26): [Ar] $3d^{10}$ $4s^1$, Cu^+: $3d^{10}$, S = 0, Cu^{2+} : $3d^9$, S = 1/2
^{63}Cu, ^{65}Cu : I = 3/2 (100 %) 2I+1 = 4 EPR lines

Tetrahedral

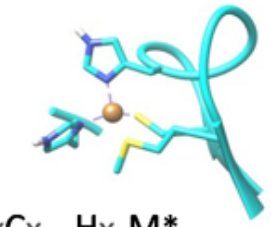

$HxCx_{2-4}Hx_4M^*$

Distorted tetrahedral

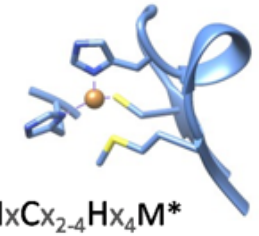

$HxCx_{2-4}Hx_4M^*$

Distorted tetragonal

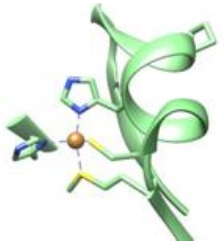

$HxCx_{4-8}Hx_4M^*$

	g values	A values [$\times 10^{-4}$ cm^{-1}]
azurin	$g_x = 2.032$	$A^{Cu}_x = 7$
	$g_y = 2.056$	$A^{Cu}_y = 7$
	$g_z = 2.259$	$A^{Cu}_z = 58$
rusticyanin	$g_x = 2.020$	$A^{Cu}_x = 64$
	$g_y = 2.062$	$A^{Cu}_y = 9$
	$g_z = 2.217$	$A^{Cu}_z = 56$
AcoP	$g_x = 2.019$	$A^{Cu}_x = 65$
	$g_y = 2.057$	$A^{Cu}_y = 12$
	$g_z = 2.193$	$A^{Cu}_z = 66$

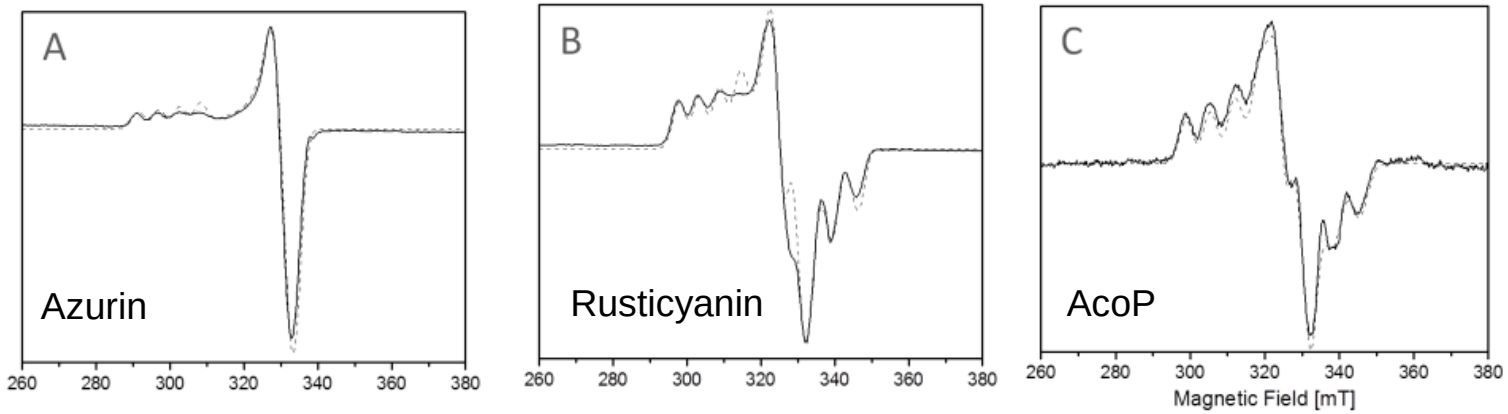

15 K, 9.4 GHz, pH 5.0

More than half-filled d orbitals:
$g_{x,y,z} > 2.0023$

Full or partial resolution of the hyperfine lines

See practical session P2 (Biomimetic Cu complex)

Roger *et al.*, PLOS One (2014)

This project has received funding from the European Union's Horizon 2020 research and innovation programme under grant agreement No 101004806

Anisotropic hyperfine couplings: spectral effects

- General case: anisotropic ***g*** and ***A*** tensors

Example: Molybdenum enzymes, Mo (Z = 42): [Kr] $4d^5\ 5s^1$,
Mo^{4+} : [Kr] $4d^2$, S = 0 or 1?
Mo^{5+} : [Kr] $4d^1$, S = ½,
Mo^{6+} : [Kr], S = 0

^{95}Mo, ^{97}Mo, I = 5/2 (25 %)
^{92}Mo, ^{94}Mo, ^{96}Mo, ^{98}Mo, ^{100}Mo, I = 0 (75 %)

Less than half-filled d orbitals:
$g_{x,y,z} < 2.0023$

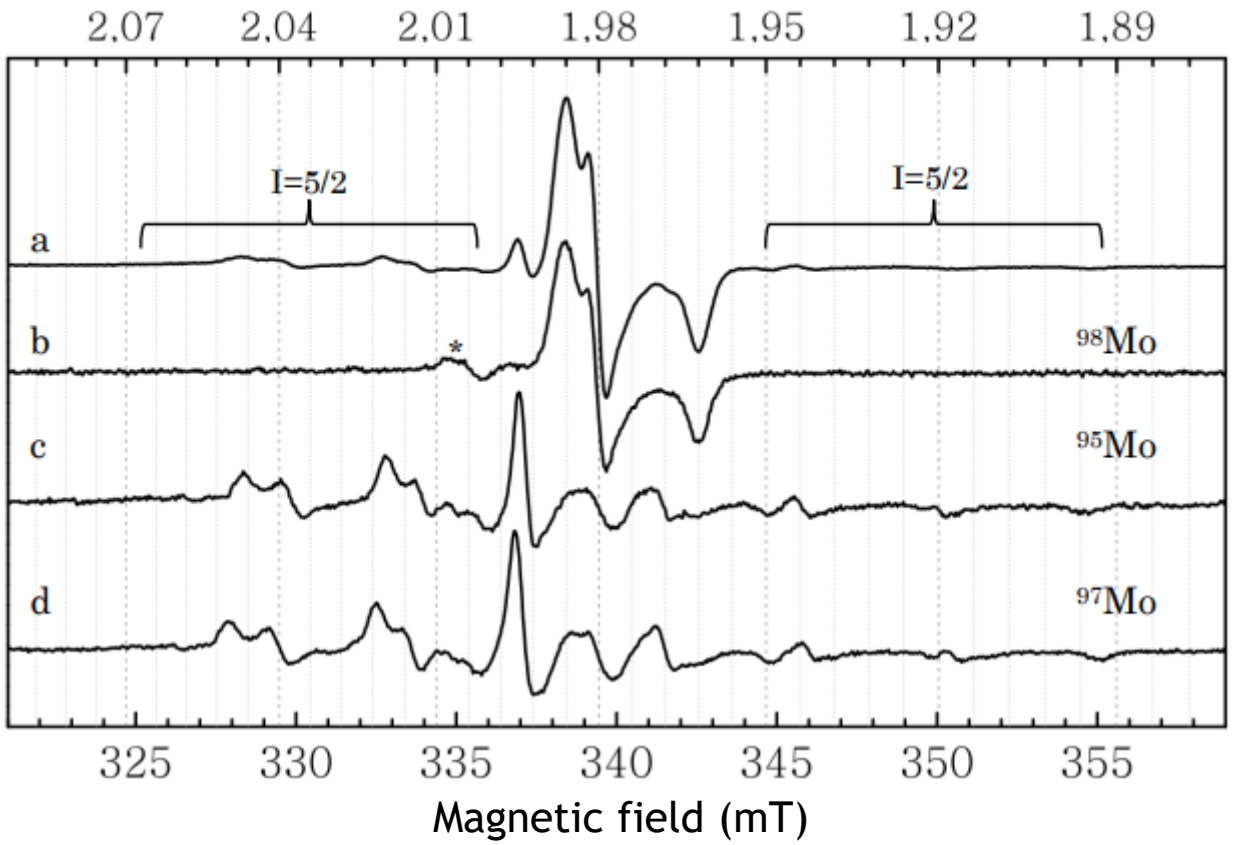

Model of the active site of *E. coli* nitrate reductase A (NarGH)

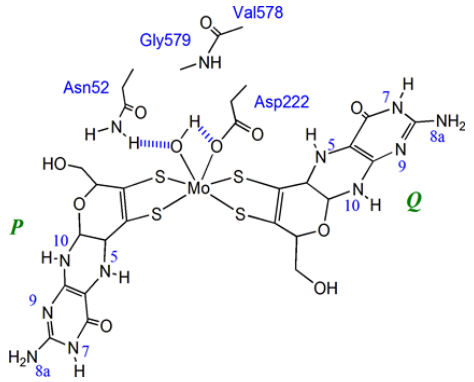

a: with naturally-abundant isotopes
b, c, d: isotopically-enriched NarGH from bacteria grown in minimal medium supplemented with Mo isotopes

Ceccaldi, P., PhD thesis, AMU (2013)

This project has received funding from the European Union's Horizon 2020 research and innovation programme under grant agreement No 101004806

Spin quantification

- Quantitative interpretation of EPR intensities

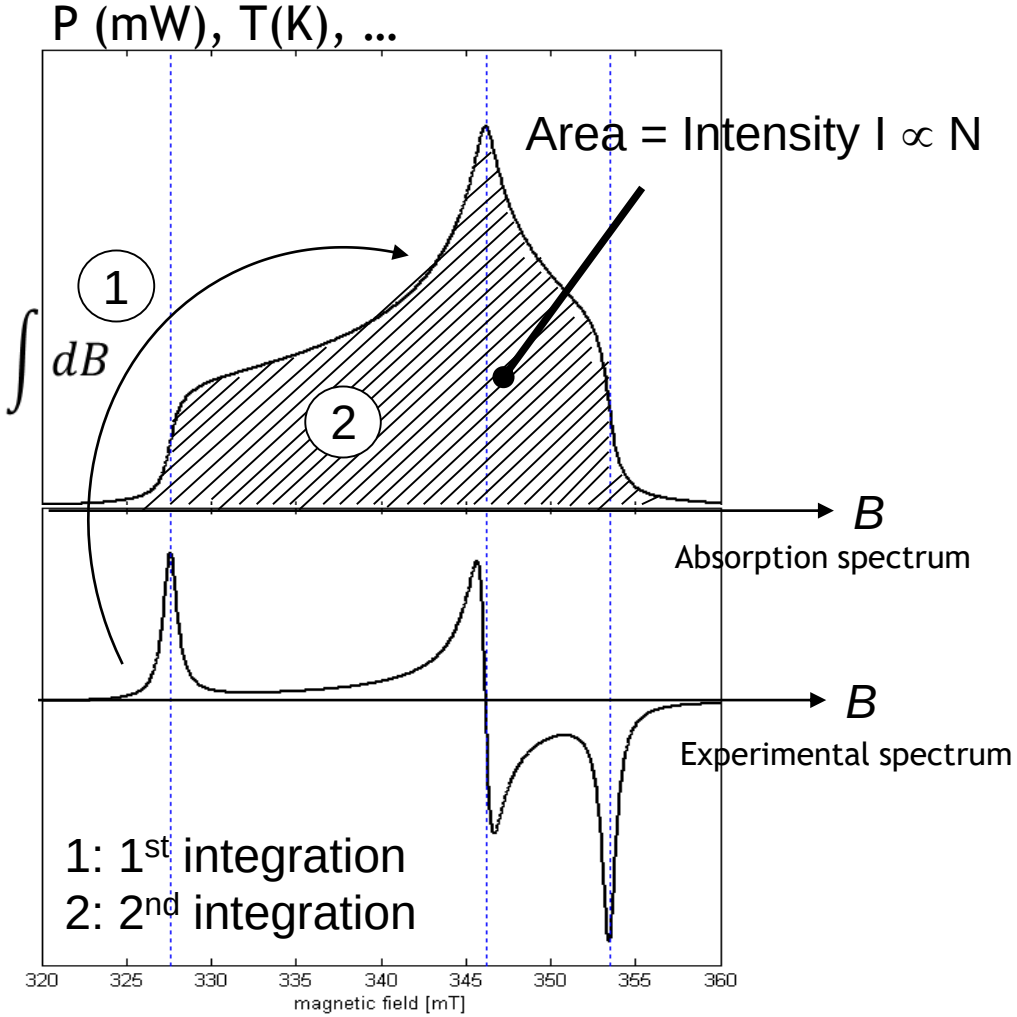

- Determination of absolute spin concentration using a reference sample e.g. copper sulfate $Cu^{II}(H_2O)_6$, S = ½, 1-10 mM

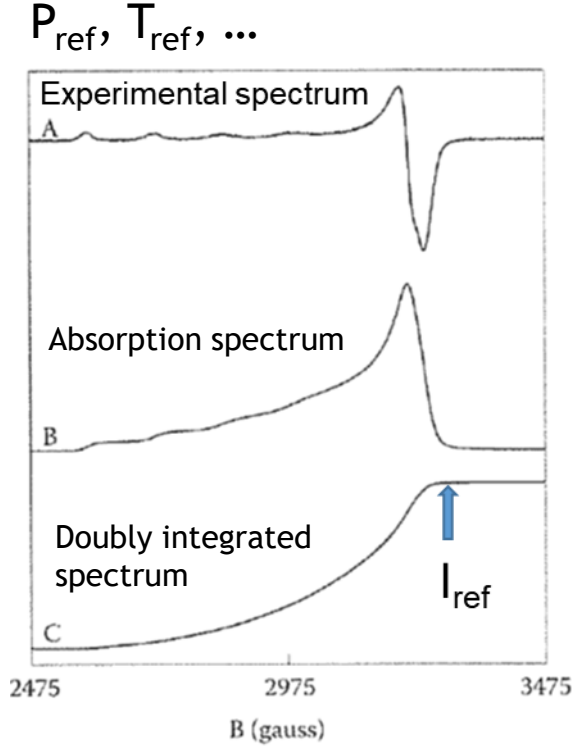

$$\frac{[Species\ X]}{[ref]} = \frac{I}{I_{ref}} \sqrt{\frac{P}{P_{ref}} \frac{T_{ref}}{T}} \ldots$$

This project has received funding from the European Union's Horizon 2020 research and innovation programme under grant agreement No 101004806

Functional characterization of metal centers

- EPR-monitored redox titrations

→ Preparing several samples in **well controlled redox states** (fixed by freezing), measuring the EPR spectra and analyzing the variation of the EPR intensities against the sample redox potential

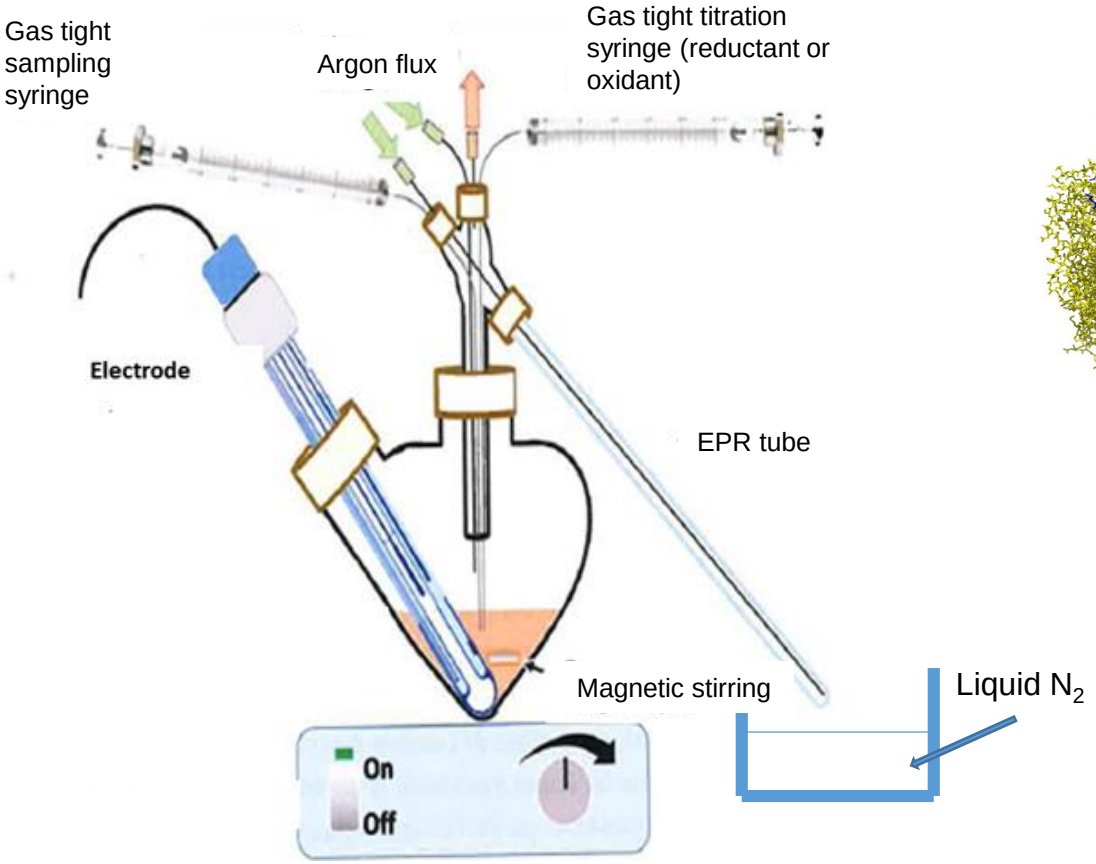

Alternative: using a glovebox

Example: E. coli nitrate reductase A NarGHI

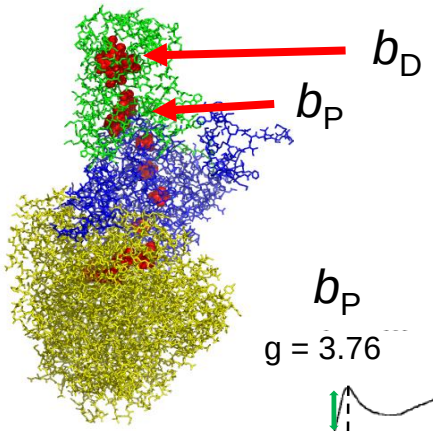

9 samples prepared at different redox potentials

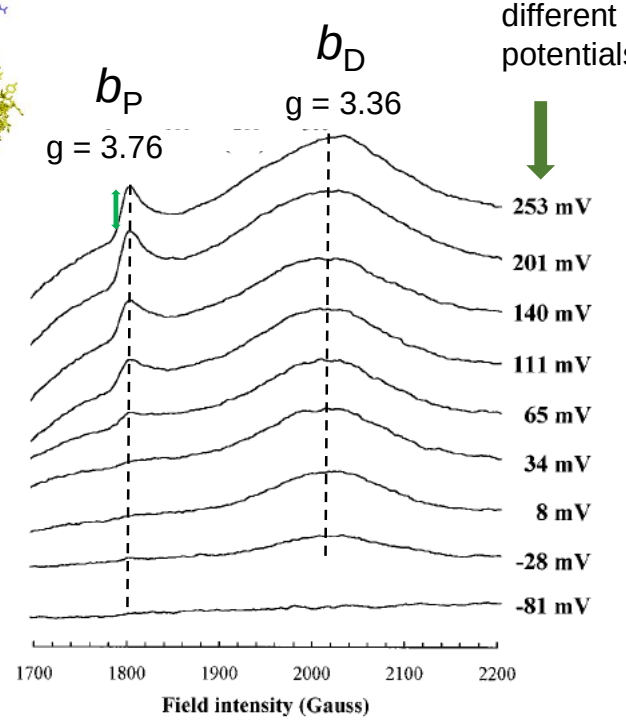

Magalon *et al.*, J Biol Chem (1997)

This project has received funding from the European Union's Horizon 2020 research and innovation programme under grant agreement No 101004806

Functional characterization of metal centers

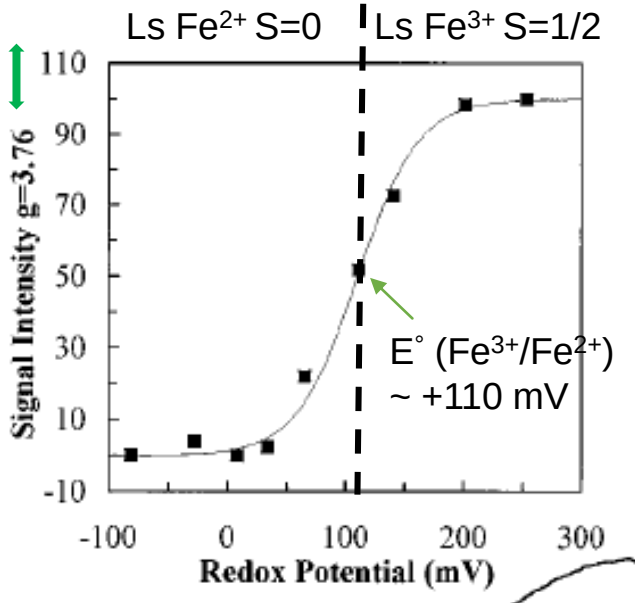

- The signal amplitude is proportionnal to [Fe^{3+}]
- The solid line corresponds to a theoretical curve obtained from the Nernst equation and fitted to the experimental points

$$I_{ox} = \frac{I_{max}}{1 + 10^{\frac{E_{ox/red} - E^0_{ox/Red}}{0.06}}}$$

- 3 typical cases:

→ Metal center with EPR-active oxidized form

→ Metal center with EPR-active reduced form

Example: [2Fe-2S] clusters

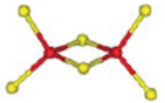

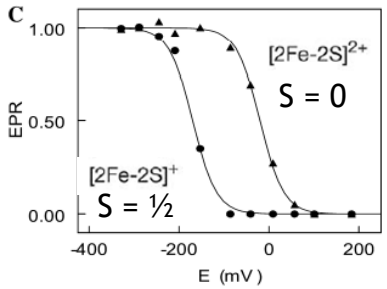

$$I_{red} = \frac{I_{max}}{1 + 10^{\frac{E^0_{ox/red} - E_{ox/red}}{0.06}}}$$

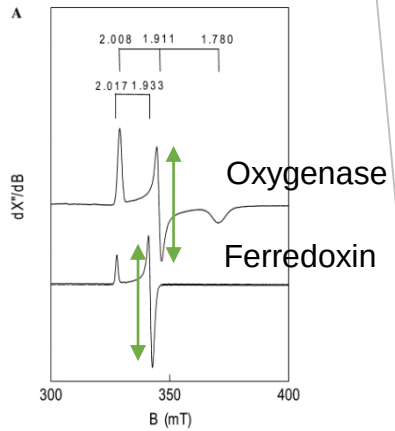

→ Metal center with three redox states and EPR-active intermediate

$Mo^{4+} \overset{E°_2}{\leftrightarrow} Mo^{5+} \overset{E°_1}{\leftrightarrow} Mo^{6+}$

Example: Mo^{VI}/Mo^{V} (S = ½)/Mo^{IV}

$$I_{int} = \frac{I_{max}}{1 + 10^{\frac{E_{ox/red} - E^0_1}{0.06}} + 10^{\frac{E^0_2 - E_{ox/red}}{0.06}}}$$

Bell-shape curve

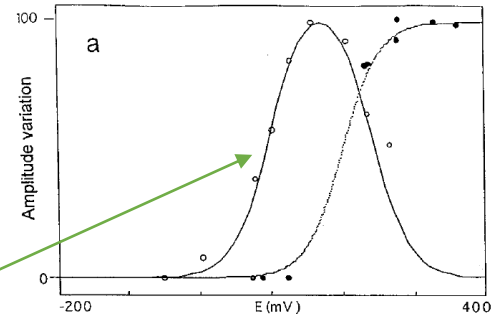

Chakraborty *et al.*, Arch Biochem Biophys (2005), Magalon *et al.*, Biochemistry (1998)

This project has received funding from the European Union's Horizon 2020 research and innovation programme under grant agreement No 101004806

Functional characterization of metal centers

- EPR-monitored binding experiments

$$M + L \rightleftharpoons ML$$

M: metal
L: ligand

$$K_a = \frac{[ML]}{[M][L]} = \frac{1}{K_d}$$

K_a : association constant

K_d : dissociation constant
(the smaller the dissociation constant, the more tightly the ligand binds)

➡ Example: Measuring the Affinity of nitrite for methemoglobin (MetHb)

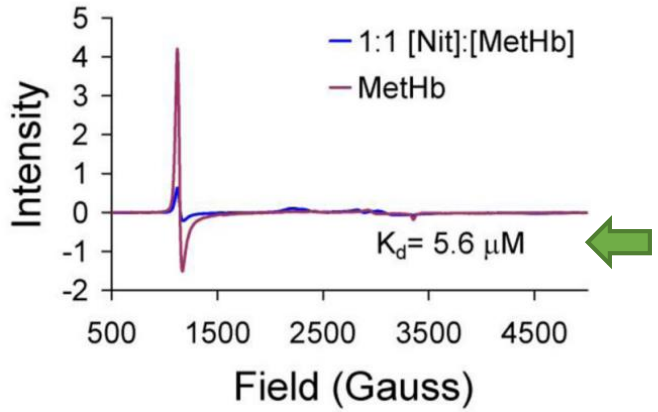

15 K, 0.8 mW

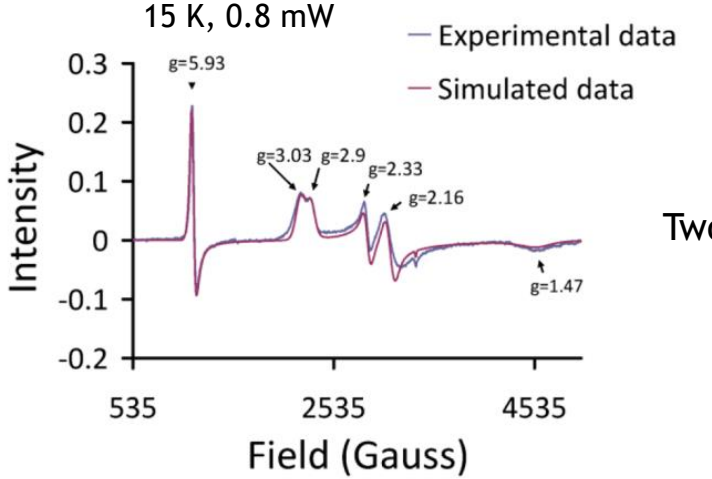

Two ls Fe^{3+} species

Goetz et al. (2010) Nitrite oxide

This project has received funding from the European Union's Horizon 2020 research and innovation programme under grant agreement No 101004806

Functional characterization of metal centers

- EPR-monitored kinetics

e.g., the formation of an intermediate when an enzyme reacts with its substrate

$i = i_{max}(1- \exp(-kt))$

- i: EPR amplitude of the product
- i_{max}: EPR amplitude of the product
- t: time
- k: 1st order rate constant

➡ Example: (Rapid) Freeze quench

Mixing 2 reagents A & B
(*e.g.*, A: enzyme, B: its substrate)

⬇

Leaving them to react for a pre-determined duration (ageing)

⬇

Mixture ejected into an isopentane solution to quench its state

⬇

Frozen particles are collected in an EPR tube

⬇

EPR spectrum is recorded at low temperature

Principle of the freeze quench

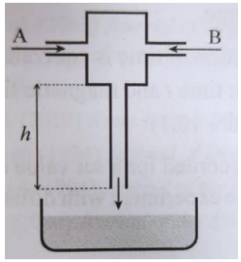

Trapping intermediates at the
millisecond time scale

EPR spectra for different reaction times of binding azide to myoglobin

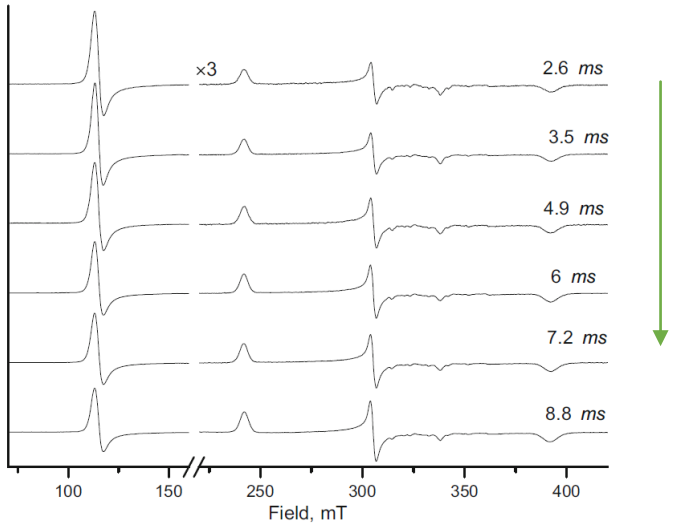

Progress of binding reaction

Nami et al. (2016) Appl Magn Reson

This project has received funding from the European Union's Horizon 2020 research and innovation programme under grant agreement No 101004806

Selective detection of metal centers in multicentre metalloproteins

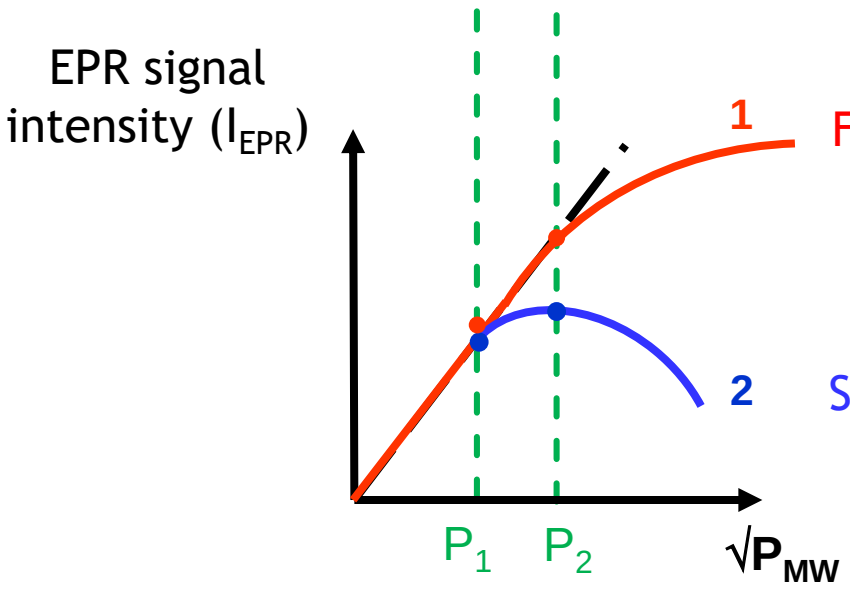

Fast relaxing centre (short T_1)

e.g., $hsFe^{3+}$, $hsCo^{2+}$, $[3Fe\text{-}4S]^{1+}$, $[4Fe\text{-}4S]^{1+}$…

Slow relaxing centre (long T_1)

e.g., $lsFe^{3+}$, $lsCo^{2+}$, Ni^{1+}, Ni^{3+}, Cu^{2+}, Mo^{5+}, W^{5+}, $[2Fe\text{-}2S]^{1+}$…

➡ Measuring spectra at two different microwave powers and making spectral differences

$P_{MW} = P_1$

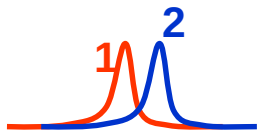

$P_{MW} = P_2$

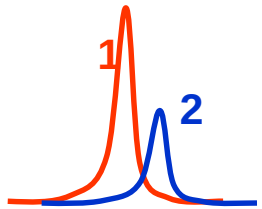

This project has received funding from the European Union's Horizon 2020 research and innovation programme under grant agreement No 101004806

Selective detection of metal centers in multicentre metalloproteins

- Relaxation broadening

Faster relaxing centre
Slower relaxing centre

« Low T »

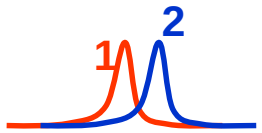

Higher T

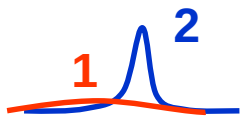

Explains why fast-relaxing metals ($hsFe^{3+}$, $hsCo^{2+}$, $[3Fe\text{-}4S]^{1+}$, $[4Fe\text{-}4S]^{1+}$,…) are not detected at room-T

- Example: separating overlapping EPR signals in *E. coli* nitrate reductase A (NarGHI)

In the same sample:

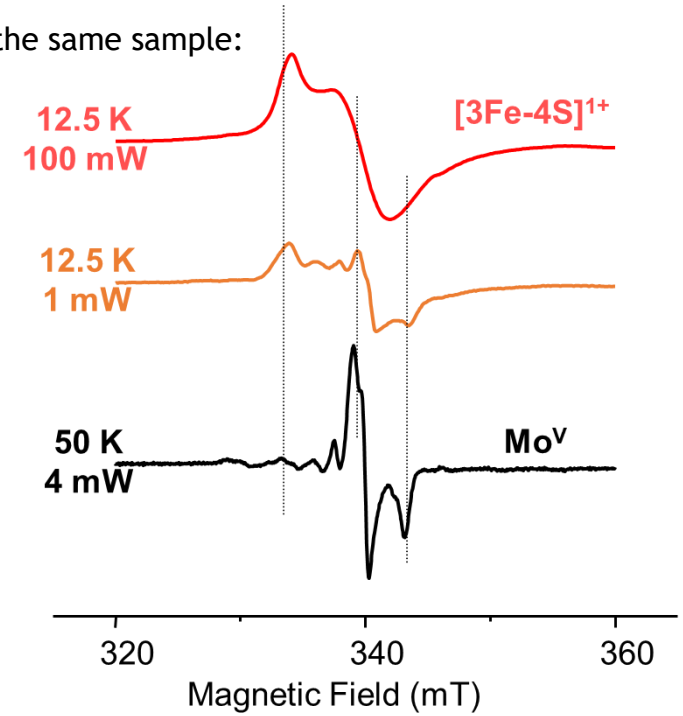

The $[3Fe\text{-}4S]^{+}$ center relaxes faster than Mo^{V} as:

→ Its EPR signal disappears first when the temperature is increased

→ It withstands the highest microwave power at a given temperature (before saturation)

See practical session P2
(Ni^{3+} and $[3Fe\text{-}4S]^{+}$ in hydrogenase)

This project has received funding from the European Union's Horizon 2020 research and innovation programme under grant agreement No 101004806

Increasing microwave frequency to enhance spectral resolution

$$h\nu = g\beta B_0$$

$$B_1 - B_2 = h\nu / \beta\,[1/g_1 - 1/g_2]$$

➡ **The resolution of the g-tensor is proportional to the microwave frequency**

- Example: Mo(V) cofactor in Aldehyde Oxidoreductase from *D. gigas*

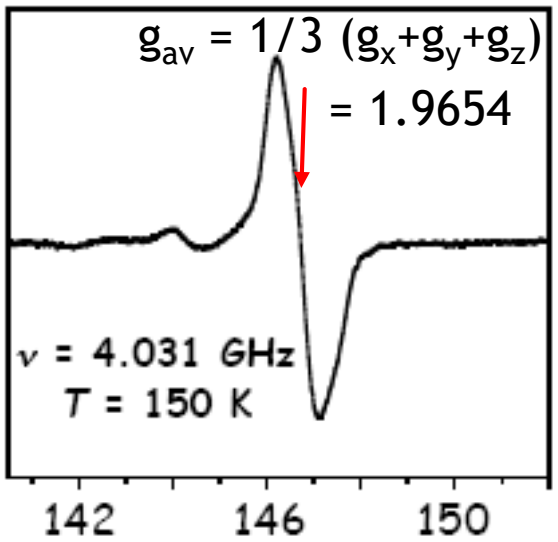

Isotropic

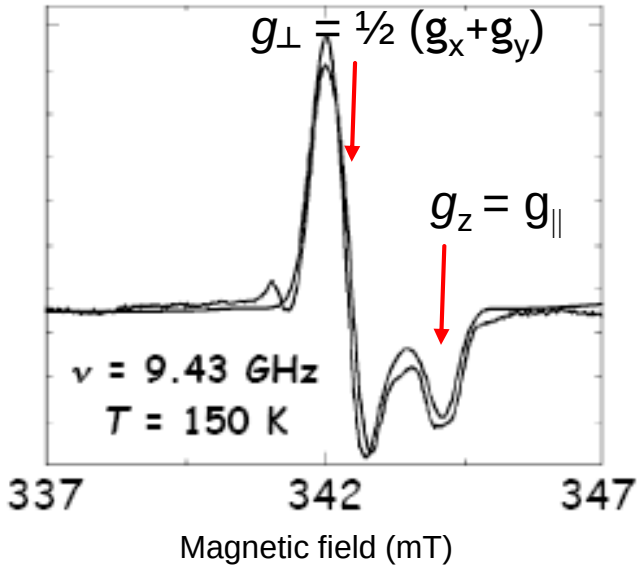

Axial

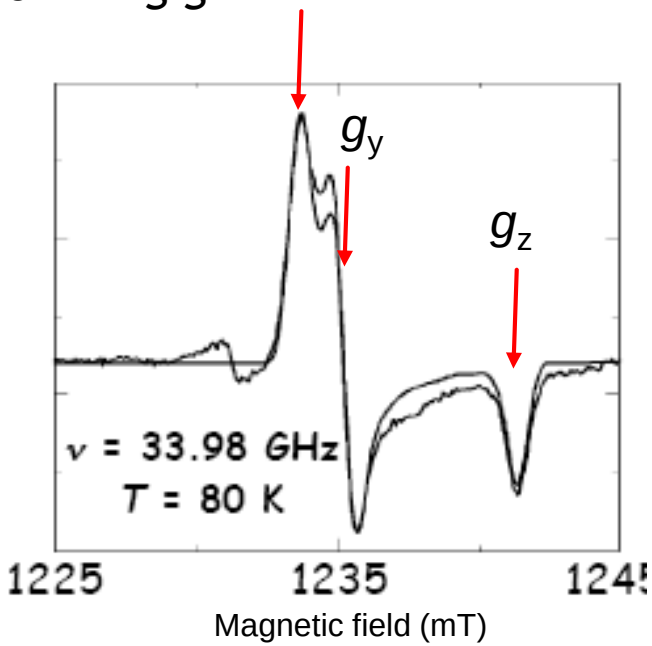

Rhombic

$g_{x,y,z}$ = 1.9703, 1.9678, 1.9581

More *et al.*, Biochemistry (1998)

This project has received funding from the European Union's Horizon 2020 research and innovation programme under grant agreement No 101004806

Complementing cw EPR with hyperfine spectroscopy

Thermus thermophilus sulfite dehydrogenase

$$HSO_3^- + H_2O \rightleftharpoons SO_4^{2-} + 2e^- + 3H^+$$

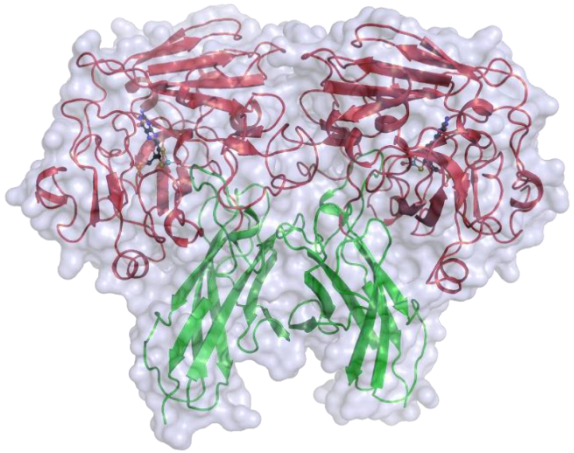

+ 1.8 M Na_3PO_4

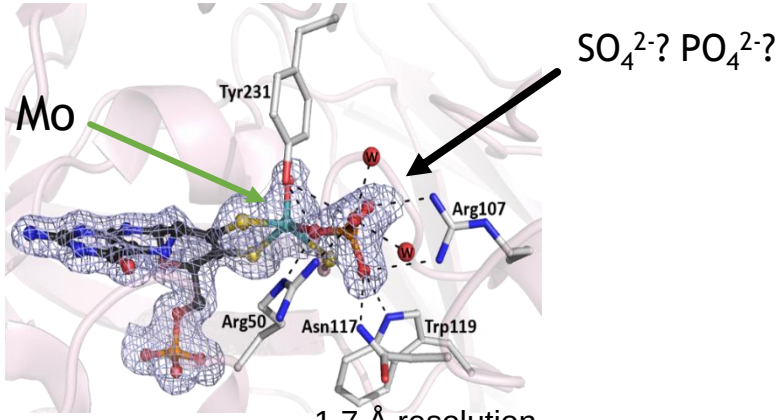

1.7 Å resolution

Simulation of HYSCORE spectrum allows to unambiguously assign the splitting seen by cw EPR to a hyperfine coupling with a directly coordinated phosphate molecule with (A_x, A_y, A_z) (^{31}P) ≈ (22, 21, 29) MHz

9.4803 GHz, 70 K, 0.1 mT, 1 mW

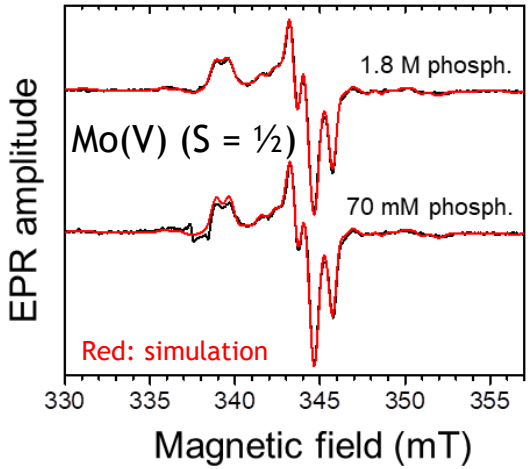

(g_x, g_y, g_z) = (1.9966, 1.9700, 1.9622)
(A_x, A_y, A_z) ≈ (22, 21, 29) MHz with I = 1/2

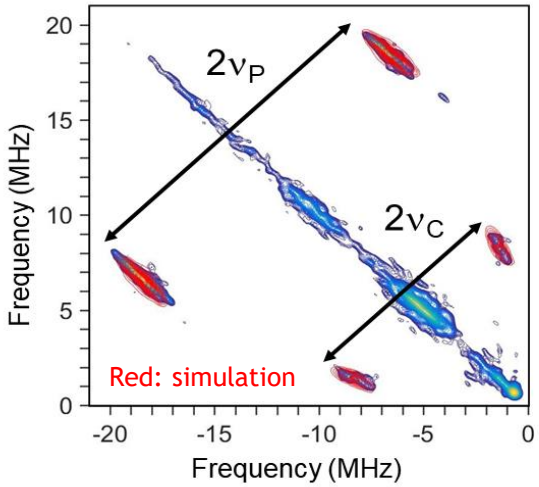

Contour plot after FFT, (-,+) quadrant 9.6980 GHz, g_2, τ = 200 ns, 50 K, 19 hours

ν : nuclear Larmor frequency (6.0 MHz and 3.8 MHz for ^{31}P and ^{13}C, resp.)

A. Djeghader et al., ChemComm. (2020)

This project has received funding from the European Union's Horizon 2020 research and innovation programme under grant agreement No 101004806